Proceedings of Computational Engineering Conference JSCES
Vol. 28, 2023 May

Corrected ALE-ISPH with novel Neumann boundary condition and density-based particle shifting technique

Daniel S. Morikawa [1)] , Kumpei Tsuji [2)] and Mitsuteru Asai [3)]

[1)]Ph.D., JAMSTEC (3173-25, Showa-machi, Kanazawa-ku, Yokohama-city, Kanagawa, E-mail: morikawad@jamstec.go.jp)
[2)]Ph.D., Tohoku University (980-8579, 6-6-06 Aramaki Aoba, Aoba-ku, Sendai-city, Miyagi, E-mail: kumpei.tsuji.e1@tohoku.ac.jp)
[3)]Ph.D., Kyushu University (819-0395, 744 Motooka Nishi-ku, Fukuoka, E-mail: asai@doc.kyushu-u.ac.jp)

Correction in the gradient and Laplacian operators have the potential to drastically increase the accuracy of the Smoothed Particle Hydrodynamics (SPH) at the expense of computational stability. This paper proposes a stable implementation of such corrections in all derivative operators to the Arbitrary Lagrangian Eulerian incompressible SPH (ALE-ISPH) method. To solve the problem of instability, we have developed a novel density-based particle shifting technique (PST) that uses the numerical density as a critical constraint variable to maintain the fluid's overall volume for the whole simulation. In addition, we propose a novel Neumann boundary condition (BC) applied directly on the velocity, which increases the accuracy even further. The method has been verified and validated, and, at last, we show an application of the method for surface tension problems.

Key Words : *ISPH, ALE, Particle Shifting Technique, Surface Tension*

1. INTRODUCTION

Since its conception, the Smoothed Particle Hydrodynamics (SPH; [1,2]) have been greatly improved over the years in terms of numerical accuracy. Highlighting this improvements we have the correction of kernel gradient [3,4] and Laplacian operator [5].

The use of such corrections in purely Lagrangian description of SPH causes particles to move along streamlines, which leads to particle clustering, an intrinsic problem of particle methods. This results in anisotropic particle configurations within the compact support, which degrade the accuracy of the kernel interpolation of the SPH method. Particle Shifting Techniques (PST), firstly proposed by [6], prevent anisotropic particle configuration by slightly shifting the particle position and realigning the particles regardless of the Lagrange velocity. It is an effective method to solve the problem of particle clustering. Examples of particle shifting techniques can be found on [7,8,9].

However, current PSTs do not shift if the particle configuration in the compact support is nearly isotropic. Therefore, even if the particle configuration becomes increasingly sparse, it will not be shifted if the configuration is considered isotropic, resulting in a gradual expansion of the overall volume. In our opinion, the discussion of volume conservation by PST is not well discussed. In this paper, we propose a new PST specifically designed to impose volume conservation on incompressible fluids. Given that we use the numerical density of the particle to evaluate volume conservation, we call this technique Density-based Particle Shifting.

Another contribution of this paper is related to boundary conditions (BC). A widely used method of wall boundary conditions for particle simulations is the Fixed Wall Ghost Particles (FWGPs) (e.g. [10,11]). This method satisfies the wall BCs by placing ghost particles inside the wall boundary and applying the desired BC on them, usually treating the wall particles as an extension of the fluid (i.e., interpolating pressure and velocity over the wall particles). As a result, it is usually necessary to include several layers of wall particles to satisfy the unity condition. Here, we propose a novel Neumann boundary condition on the wall particles that perfectly satisfy the non-penetration BC in a single layer wall particles, applying it directly on the velocity.

2. ISPH PROJECTION IN ALE DESCRIPTION

Let us start with the Navier–Stokes and continuity equations for incompressible fluid in the ALE description

$$\frac{\partial \mathbf{v}}{\partial t} + \mathbf{c} \cdot \nabla \mathbf{v} = -\frac{1}{\rho_0} \nabla p + \nu \nabla^2 \mathbf{v} + \mathbf{g}, \tag{1}$$

$$\nabla \cdot \mathbf{v} = 0. \tag{2}$$

In ALE description, the material point (particle) moves according to an arbitrary reference velocity called transport velocity, here represented by $\mathbf{w}$. In the above equations, $\mathbf{v}$ is the Lagrangian fluid velocity, $\mathbf{c}$ is the relative velocity $\mathbf{c} = \mathbf{v} - \mathbf{w}$, p is the fluid pressure, ν is the kinematic viscosity, $\mathbf{g}$ is the gravity acceleration and ρ_0 is the reference fluid density.

Following the traditional projection method [12,13,14], Eq. 1 is split into a predictor step

$$\mathbf{v}^* = \mathbf{v}^n + \Delta t \left(\nu \nabla^2 \mathbf{v}^n + \mathbf{g} - \mathbf{c}^n \cdot \nabla \mathbf{v}^n \right) \tag{3}$$

and a corrector step

$$\mathbf{v}^{n+1} = \mathbf{v}^{*} - \Delta t\Big(\frac{1}{\rho_0}\nabla p^{n+1}\Big), \tag{4}$$

where superscripts n, $*$ and $n+1$ represent the current, predictor and next steps, respectively.

To obtain the pressure Poisson equation, one must multiply both sides of the corrector step (Eq. 4) by ∇ and, considering the incompressible condition (Eq. 2) for $n+1$ step, we may find, after rearranging,

$$\nabla^2 p^{n+1} = \frac{\rho_0}{\Delta t}\nabla \cdot \mathbf{v}^{*}. \tag{5}$$

Finally, one must calculate the transport velocity $\mathbf{w}^{n+1}$ and update the particle position as

$$\mathbf{x}^{n+1} = \mathbf{x}^{n} + \Delta t \mathbf{w}^{n+1}. \tag{6}$$

Probably the most important advantage of ALE formulation is its versatility in terms of adapting to different situations. For instance, one may chose the transport velocity $\mathbf{w}$ equals to the Lagrangian velocity $\mathbf{v}$ and retrieve back the Lagrangian formulation. Another option is, for steady flows, for example, chose $\mathbf{w} = 0$, so it becomes an Eulerian formulation. In a more gereral case, following [15], the transport velocity is calculated as

$$\mathbf{w}^{n+1} = \mathbf{v}^{n+1} + \frac{1}{\Delta t}\delta\mathbf{r}_{\text{shift}}, \tag{7}$$

where $\delta\mathbf{r}_{\text{shift}}$ is a small shifting of the particle position with the objective of leading to a better particle distribution ($|\delta\mathbf{r}_{\text{shift}}/\Delta t| << |\mathbf{v}|$).

3. SPH OPERATORS

Here, we summarize the SPH operators used in this study. All formulas are derived from the the original SPH approximations [1,2] for an arbitrary function f

$$\langle f\rangle_i = \sum_j^N \frac{m_j}{\rho_j} f_j W(\mathbf{r}_{ij}, h), \tag{8}$$

where, m represents the mass, W is the SPH weight function, $\mathbf{r}$ is the relative position, h is the smoothing length (in our code, $h = 1.2d$, d being the particle diameter), N is the total number of particles, $\langle\rangle$ represents the SPH approximation and the subscripts i and j represent target and neighboring particle, respectively. To simplify the notation, we abbreviate $W(\mathbf{r}_{ij}, h)$ as W_{ij} and $\nabla W(\mathbf{r}_{ij}, h)$ as ∇W_{ij}.

In this study, the correction of kernel gradient [3,4] is calculated as

$$\langle\nabla f\rangle_i = \sum_j^N \frac{m_j}{\rho_j}(f_j - f_i)\mathbf{L}_i\nabla W_{ij}, \tag{9}$$

where

$$\mathbf{L}_i = \Big(\sum_j \frac{m_j}{\rho_j}\nabla W_{ij}\otimes\mathbf{r}_{ji}\Big)^{-1}. \tag{10}$$

We use the Laplacian operator derived from [5], which, after some rearranging of the original equation, can be caculated as

$$\langle\nabla^2 f\rangle_i = \sum_j^N A^{*}_{ij}(f_i - f_j), \tag{11}$$

where

$$A^{*}_{ij} = A_{ij} + \Big(\sum_j^N A_{ij}\mathbf{r}_{ij}\Big)\cdot\frac{m_j}{\rho_j}\tilde{\nabla}W_{ij}, \tag{12}$$

$$A_{ij} = \mathbf{B}_i : \frac{2m_j}{\rho_j}\frac{\mathbf{r}_{ij}\nabla W_{ij}}{\mathbf{r}^2_{ij}}. \tag{13}$$

and

$$\mathbf{B}_i : \Big[\sum_j^N \frac{m_j}{\rho_j}\mathbf{r}_{ij}\mathbf{e}_{ij}\mathbf{e}_{ij}\nabla W_{ij} + \Big(\sum_j^N \frac{m_j}{\rho_j}\mathbf{e}_{ij}\mathbf{e}_{ij}\nabla W_{ij}\Big)\cdot \mathbf{L}_i\cdot\Big(\sum_j^N \frac{m_j}{\rho_j}\mathbf{r}_{ij}\mathbf{r}_{ij}\nabla W_{ij}\Big)\Big] = -\mathbf{I}. \tag{14}$$

Here, $\mathbf{e}_{ij} = \mathbf{r}_{ij}/|\mathbf{r}_{ij}|$. For more details on the formulations and the rearranging of the Laplacian operator, please refer to [16].

4. BOUNDARY CONDITIONS

For the wall, we use fixed wall ghost particles (FWGPs) to represent the wall surface. In this method, the wall is represented by a single layer wall ghost particles located behind the wall surface. Hence, to describe each particle, it is necessary to provide its location and normal direction $\mathbf{n}$ of the wall surface that it represents.

(1) Slip/non-slip boundary conditions

First, we show the application of boundary conditions for the predictor step, that is, considering either slip or non-slip condition. Let us start with the viscous term of the Navier–Stokes equations already discretized with the SPH approximation:

$$\langle\nu\nabla^2\mathbf{v}\rangle_i = \sum_j^N \frac{\nu_i + \nu_j}{2}A^{*}_{ij}(\mathbf{v}_i - \mathbf{v}_j). \tag{15}$$

Then, enforcing the slip/non-slip condition is equivalent to find the value of $\mathbf{v}_j$ (for $j \in$ wall) that satisfies this condition. Here, we solve this problem with two simple rules:

- For non-slip condition: $\mathbf{v}_j = \mathbf{v}_{\text{wall}}$;
- For slip condition: $\mathbf{v}_j = \mathbf{v}_i$.

(2) Novel Neumann boundary condition

We developed a novel Neumann boundary condition in which the non-penetration condition is enforced directly on the pressure value of wall particles. Let us multiply the corrector step (Eq. 4) on both sides by the unity normal direction vector of a wall surface $\mathbf{n}$

$$\mathbf{v}^{n+1}\cdot\mathbf{n}=\Big[\mathbf{v}^{*}-\Delta t\Big(\frac{1}{\rho_0}\nabla p^{n+1}\Big)\Big]\cdot\mathbf{n}. \tag{16}$$

The imposition of the non-penetration condition requires to solve Eq. 16 substituting $\mathbf{v}^{n+1}$ by the real wall velocity $\mathbf{v}_{\text{wall}}$. Notice that the target particle of this equation is a wall particle. After rearranging the pressure to the left-hand side and applying the non-penetration BC, we find

$$\nabla p^{n+1}\cdot\mathbf{n}=\frac{\rho_0}{\Delta t}(\mathbf{v}^{*}-\mathbf{v}_{\text{wall}})\cdot\mathbf{n}. \tag{17}$$

(3) PPE including boundary conditions

Succinctly, pressure calculation including free-surface (FS) and non-penetration boundary conditions can be summarized as the following equations:

$$\begin{cases} p_i^{n+1}=0, & \text{if } i\in \text{FS}\\ \nabla p_i^{n+1}\cdot\mathbf{n}_i=\frac{\rho_0}{\Delta t}\mathbf{v}_i^{*}\cdot\mathbf{n}_i, & \text{if } i\in \text{wall}\\ \nabla^2 p_i^{n+1}=\frac{\rho_0}{\Delta t}\nabla\cdot\mathbf{v}_i^{*}, & \text{if } i\in \text{fluid}\end{cases} \tag{18}$$

Applying the SPH operators for the gradient (Eq. 9) and Laplacian (Eq. 11) of p_i^{n+1}, respectively, we derive a system of linear equations with asymmetrical coefficients, given that the equations used for target wall and fluid particles are different. In this study, we use the well-known Biconjugate Gradient Stabilized (BICCGSTAB) method to solve it.

5. DENSITY-BASED SHIFTING TECHNIQUE

We developed a novel particle shifting technique (PST) that can reliably be applied in the context of incompressible fluids. The objective of the proposed PST is to address three existing problems: lead to an evenly distributed particle continuum (a), avoid particle clumping (b), and maintain overall numerical density (c).

In SPH, the numerical density is usually calculated with Eq. 8 directly. However, since we are using only one layer of wall particles, this equation would lead to lower number densities near the wall surface. To compensate that, we propose using Eq. 8 applied to a small influence radius $d^{*}_{\text{inf}}=(1.1\sqrt{\text{D}})d$, where D is the number of dimensions. Let us call the domain of neighboring particles within the small influence radius as S^{*}. Then, to compensate the smaller influence radius, we multiply Eq. 8 by a fixed parameter β, which leads to $\rho_i=\rho_0$ for a grid particle distribution. In Mathematical terms,

$$\langle\rho\rangle_i=\beta\sum_{j\in S^{*}}^{N}m_jW_{ij}, \tag{19}$$

where dist(i,j) is a function that returns the distance between points i and j. For the cubic spline with $h=1.2d$, in three-dimensions, $\beta\approx 1.028$.

Then, our proposed shifting equation can be written as

$$\delta\mathbf{r}_{\text{shift},i}=C_{\text{shift}}h\Big(\delta\mathbf{r}_{\text{w},i}+\delta\mathbf{r}_{\text{dens},i}\Big), \tag{20}$$

where

$$\delta\mathbf{r}_{\text{w},i}=\begin{cases}\delta\mathbf{r}^{*}_{\text{w},i}-(\delta\mathbf{r}^{*}_{\text{w},i}\cdot\mathbf{N}_i)\mathbf{N}_i, & \text{if } i\in\text{FS}\\ \delta\mathbf{r}^{*}_{\text{w},i}, & \text{otherwise}\end{cases}, \tag{21}$$

$$\delta\mathbf{r}^{*}_{\text{w},i}=\sum_{j\in S^{*}}^{N}\Big(\frac{m_j}{\rho_j}W_{ij}\Big)\mathbf{e}_{ij}, \tag{22}$$

and

$$\delta\mathbf{r}_{\text{dens},i}=\sum_{j\in S^{*}}^{N}\Big(\frac{\langle\rho\rangle_i}{\rho_0}-1+\frac{\langle\rho\rangle_j}{\rho_0}-1\Big)\mathbf{e}_{ij}. \tag{23}$$

In Eq. 20, C_{shift} is a constant shifting parameter, the $\delta\mathbf{r}_{\text{w},i}$ term aims to solve problems (a) and (b), while $\delta\mathbf{r}_{\text{dens},i}$ was designed specifically to solve problem (c). Here, $\mathbf{N}_i$ is calculated as [8]

$$\mathbf{N}_i=\frac{\mathbf{N}^{*}_i}{|\mathbf{N}^{*}_i|}, \tag{24}$$

$$\mathbf{N}^{*}_i=\sum_{j}^{N}\frac{m_j}{\rho_j}(\lambda_j-\lambda_i)\tilde{\nabla}W_{ij}, \tag{25}$$

where λ_i is the minimum eigenvalue of $\mathbf{L}_i^{-1}$.

6. NUMERICAL EXAMPLES

(1) Verification: Poisenuille Flow

This example is to test the proposed method wall boundary conditions. The pipe model is illustrated in **Fig.1**(a), with dimensions $L=0.002$ m and wall particles positioned at r (radial distance from the center) equals $R=0.0005$ m. We have selected the Eulerian framework for this problem. In this way, the inlet/outlet conditions are reduced to fixed Dirichlet pressure conditions (here we chose $\Delta p=1$ Pa).

All particles are initiated with null pressure and velocity. We simulate this problem with three particle sizes: $d=6.25\times10^{-5}, 5\times10^{-5}$ and 2×10^{-5} m. Because of the novel Neumann BC and [5]'s Laplacian correction applied to the viscous term of the Navier–Stokes equation (Eq. 1), the results for x velocity become basically indistinguishable from the theoretical solution (as seen in **Fig.2**) for all three cases.

(2) Validation: Rotating Square Patch

This example was first proposed by [17]. A 2D square fluid is centered at the origin (0, 0) and an initial velocity $(\omega y,-\omega x)$ is applied to all particles without the presence of gravity. Then, the fluid rotates and stretches in the direction of its corners, which generates a negative pressure. Here, we have chosen a square of size $L=1$ m, particle size of $d=0.02$ m and angular velocity of $\omega=1\ \text{s}^{-1}$. The objective of this example is to test the proposed density-based PST under an unfavorable situation (negative pressure). The shifting coefficient is set to $C_{\text{shift}}=0.005$.

First, **Fig.3** shows that the proposed corrected ISPH method is not stable without the application of any PST.

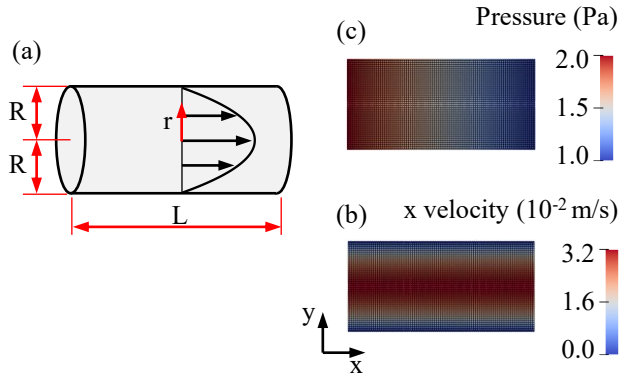

Fig. 1 Poisenuille flow: definition of geometrical variables(a) and snapshots at 0.5 s for pressure field (b) and x velocity (c)

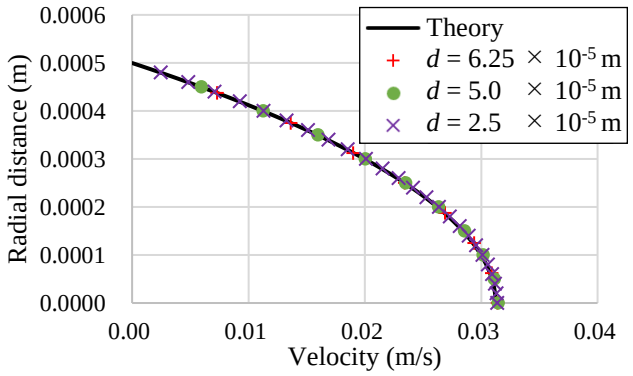

Fig. 2 Poisenuille flow: graphical results at 0.5 s for different particle sizes comparing with the theoretical solution

However, as observed in **Fig.4**, we demonstrate that the proposed density-based PST is capable of solving this problem in a very stable manner for an extended period of time. Next, as illustrated in **Fig.5**, we conclude that our proposed density-based PST is more suitable than [9]'s OPS in terms of stabilizing the free-surface and maintaining the numerical density. Lastly, the resulting pressure at the center from our proposed corrected ISPH with density-based PST is more stable than [15]'s, since it does not show any relevant oscillatory behavior. Also, our results are almost indistinguishable from [18]'s reference pressure results at the center.

(3) Application: Surface Tension

The last numerical test is the application of the proposed method to surface tension problems. Here we selected a conventional macroscopic approach to surface tension, which is calculated as

$$\mathbf{f}_i^{\mathrm{ST}} = -\sigma\kappa_i\delta\mathbf{N}_i, \tag{26}$$

where σ, κ, δ and $\mathbf{N}$ are surface tension coefficient, curvature, coefficient of unit conversion and normal direction vector, respectively. In general, curvature is calculated as half of the divergence of normal direction. However, by

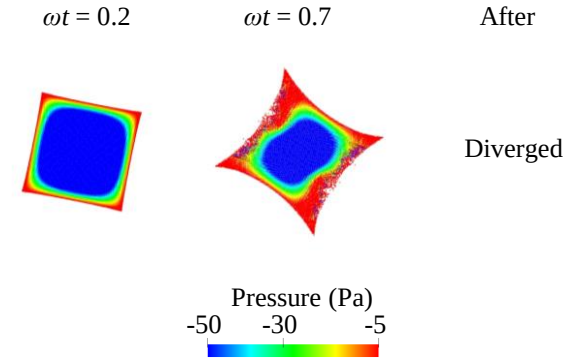

Fig. 3 Rotating square patch: resulting pressure field with the proposed corrected SPH and without any PST for different time steps

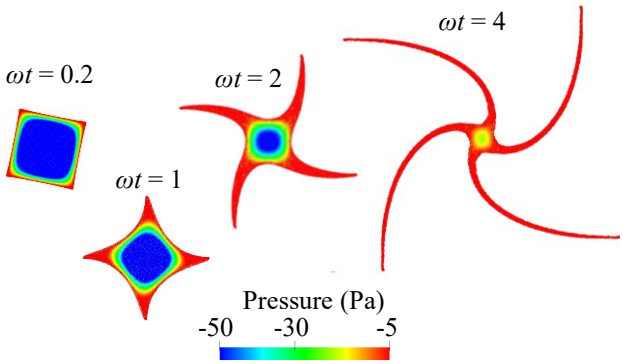

Fig. 4 Rotating square patch: resulting pressure field with the proposed corrected SPH and density-based PST for different time steps

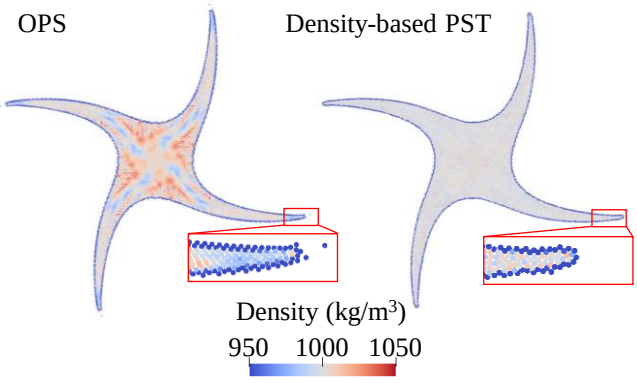

Fig. 5 Rotating square patch: resulting numerical density field with the proposed corrected SPH using OPS [9] and proposed density-based PST for $\omega t = 2$

personal experience, we substituted this "half" coefficient by 0.41, leading to

$$\kappa_i = 0.41 \sum_{j\in \mathrm{FS}}^{N_{\mathrm{FS}}} \frac{m_j}{\rho_j}(\mathbf{N}_j - \mathbf{N}_i)\cdot\mathbf{L}_i\nabla W_{ij}, \tag{27}$$

where FS refers to the domain of neighboring free-surface particles. Notice that this force is only applied to free-

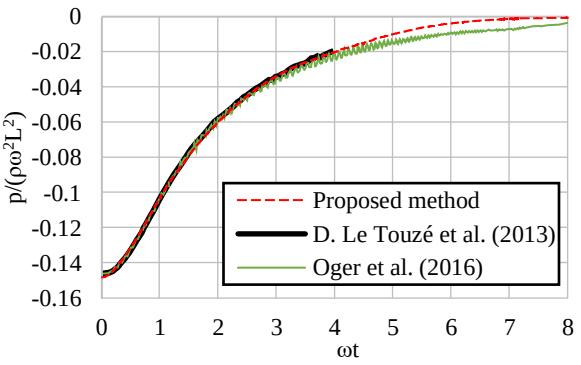

Fig. 6 Rotating square patch: time series of pressure at (0,0) comparing the proposed method (using density-based PST) with [15] and [18]

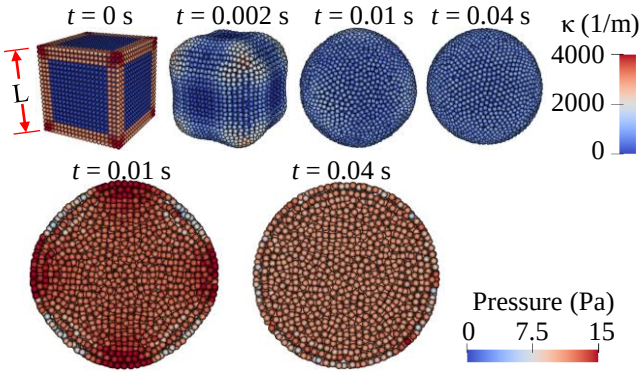

Fig. 7 Cube with surface tension: snapshots of several time steps ($L = 0.002$ m and $d = 0.0001$ m)

surface particles. δ is also chosen based on personal experience, and it is considered a fixed value of $\delta = 0.1/d$. Then, the surface tension force is included in the predictor step as an external force. Also, the Dirichlet boundary condition of free-surface particles changes as the surface tension promotes a pressure value of $2\sigma\kappa_i$.

The first example consists of a cubic fluid with size L under no gravity. σ is fixed as 0.007 N/m, and we conducted several tests with several values of d and L. **Fig.7** shows some screen shots of this simulation for 3D and centered cross-section views at different time steps. Notice that both the curvature and pressure fields are reasonably smooth. Next, on **Fig.8**, we plot 9 results with several values of d and L, showing that the solution agrees with the Laplace pressure, which is given by $2\sigma/R$, where R is the radius of the sphere.

Lastly, we include the simulation of a cuboid droplet of dimensions $2L \times 2L \times L$ (length, depth and height, respectively) initially located on a ceiling. The droplet is under the gravity acceleration of 5 m/s^2, which is counterbalanced only by the surface tension force. Also, we include the concept of contact angle (θ) simply modifying the normal direction vector **N** as shown in **Fig.9**. In this way, the resulting surface tension from that enforced contact angle automatically generates the correct forces.

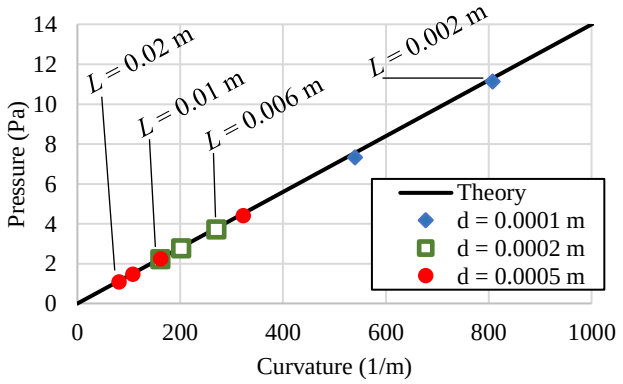

Fig. 8 Cube under surface tension: graphical results of the average pressure over curvature comparing with the theoretical Laplace pressure for various values of L

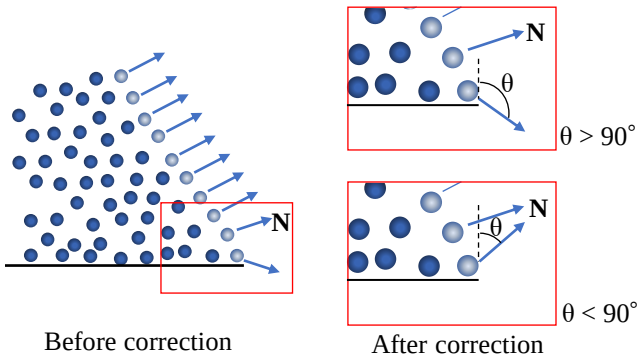

Fig. 9 Correction of the normal direction at the wall interface to enforce the desired contact angle

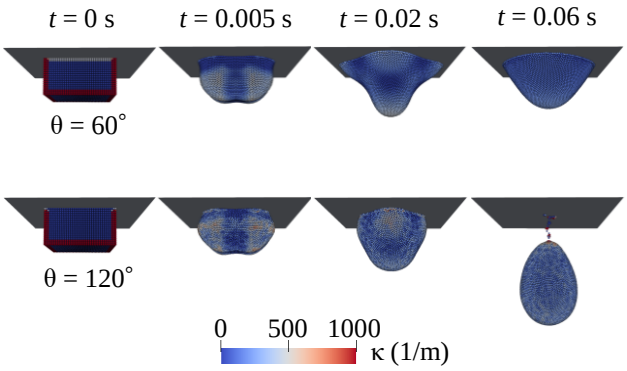

Fig. 10 Surface tension with contact angle: snapshots of several time steps of the droplet formation ($L = 0.004$ m and $d = 0.0002$ m)

Fig.10 shows the formation of the fluid droplet with two different contact angles. We chose a higher value of $\sigma = 0.07$ N/m as to generate an almost stable situation when $\theta = 60^o$. On the other hand, for $\theta = 120^o$, the surface tension forces facilitate the fall of the droplet.

7. CONCLUSION

This paper proposes a stable and accurate implementation of the SPH method using the gradient and Laplacian corrections. Then, to increase the method's accuracy and stability, we propose a novel Neumann BC for the non-penetration condition on pressure and an original density-based PST.

As a result, our proposed corrected ISPH method is capable of simulating boundary conditions accurately using only one layer of wall particles. Also, the proposed density-based PST has been tested and proved to effectively stabilize the method and maintain the numerical density of the fluid. For verification and validation, we have conducted the Poisenuille and the rotating square patch tests. Finally, we demonstrate that this numerical framework is capable of simulating surface tension problems accurately.

ACKNOWLEDGMENT This work was supported by the Japan Society for the Promotion of Science (JSPS) KAKENHI Grant Number JP-20H02418, 19H01098, and 19H00812. In addition, this study was supported by the Earthquake Research Institute (ERI) from the University of Tokyo, JURP 2021-S-B201. We also received computational environment support through the Joint Usage/Research Center for Interdisciplinary Large-scale Information Infrastructures (JHPCN) in Japan (Project ID: jh200034-NAH and jh200015-NAH).

REFERENCES

[1] Gingold, R.A. and Monaghan, J.J.: Smoothed Particle Hydrodynamics: theory and application to non-spherical stars, Astron. Soc., Vol.181, pp.375-389, 1977.

[2] Lucy, L.B.: A numerical approach to the testing of the fusion process, Astron. J., Vol.82, pp.1013-1024, 1977.

[3] Randles, P.W. and Libersky, L.D.: Smoothed particle hydrodynamics: some recent improvements and applications, Comput. Methods Appl. Mech. Engrg., Vol.139, pp.375-408, 1996.

[4] Bonet, J. and Lok, T.S.L.: Variational and momentum preservation aspects of Smoothed Particle Hydrodynamics formulations, Comput. Methods Appl. Mech. Engrg., Vol.180, pp.97-115, 1999.

[5] Faheti, R. and Manzari, M. Error estimation in smoothed particle hydrodynamics and a new scheme for second derivatives, Comput. Math. Appl. 61 (2) (2011) 482–498. doi:https://doi.org/10.1016/j.camwa.2010.11.028.

[6] Xu, R., Stansby, P. and Laurence, D. Accuracy and stability in incompressible SPH (ISPH) based on the projection method and a new approach, J. 595 Comput. Phys. 228 (2009) 6703–6725. doi:https://doi.org/10.1016/j.jcp.2009.05.032.

[7] Lind, S.J., Xu, R., Stansby, P.K. and Rogers, B.D. Incompressible smoothed particle hydrodynamics for free-surface flows: A generalised diffusion-based algorithm for stability and validations for impulsive flows and propagating waves, J. Comput. Phys. 231 (2012) 1499–1523. doi:https://doi.org/10.1016/j.jcp.2011.10.027.

[8] Sun, P.N., Colagrossi, A., Marrone, S., Antuono, M. and Zhang, A.-M. A consistent approach to particle shifting in the delta-plus-SPH model, Comput. Methods Appl. Mech. Eng. 348 (2019) 912–934. doi:https://doi.org/10.1016/j.cma.2019.01.045.

[9] Khayyer, A., Gotoh, H. and Shimizu, Y. Comparative study on accuracy and conservation properties of two particle regularization schemes and proposal of an optimized particle shifting scheme in ISPH context, J.Comput. Phys. 332 (2017) 236–256. doi:10.1016/j.jcp.2016.12.005.

[10] Colagrossi, A. and Landrini, M. Numerical simulation of interfacial flows by smoothed particle hydrodynamics, J. Comput. Phys. 191 (2003) 448–475. doi:10.1016/S0021-9991(03)00324-3.

[11] Adami, S., Hu, X. and Adams, N. A generalized wall boundary condition for smoothed particle hydrodynamics, J. Comput. Phys. 231 (2012) 7057–7075. doi:10.1016/j.jcp.2012.05.005.

[12] Chorin, A. Numerical solution of the navier-stokes equations. mathematics of computation, Math. Comput. 22 (1968) 745–762. doi:http://dx.doi.org/10.1090/S0025-5718-1968-0242392-2.

[13] Koshizuka, S. and Oka, Y. Moving-particle semi-implicit method for fragmentation of incompressible fluid, Nucl. Sci. Eng. 123 (1996) 421–434. doi:https://doi.org/10.13182/NSE96-A24205.

[14] Asai, M., Aly, A.M., Sonoda, Y. and Sakai, Y. A stabilized incompressible SPH method by relaxing the density invariance condition, J. Appl. Math., Vol.2012, 24 pages, 2012.

[15] Oger, G., Marrone, S., Touze, D.L. and Leffe, M.D. SPH accuracy improvement through the combination of a quasi-Lagrangian shifting transport velocity and consistent ALE formalisms, J. Comput. Phys. 313 (2016) 76–98. doi:https://doi.org/10.1016/j.jcp.2016.02.039.

[16] Morikawa, D.S., Tsuji, K. and Asai, M. Corrected ALE-ISPH with novel Neumann boundary condition and density-based particle shifting technique, J. Comput. Phys. X. (2023). doi: https://doi.org/10.1016/j.jcpx.2023.100125.

[17] Colagrossi, A. A meshless lagrangian method for free-surface and interface flows with fragmentation, PhD thesis, Universita di Roma La Sapienza (2005).

[18] Touze, D.L., Colagrossi, A., Colicchio, G. and Greco, M. A critical investigation of smoothed particle hydrodynamics applied to problems with free-surfaces, Int. J. Numer. Methods Fluids 73 (2013) 660–691. doi:https://doi.org/10.1002/fld.3819.